Thermodynamic and experimental study of cobalt-based alloys designed to contain TiC carbides

Patrice Berthod*, Mira Khair

Institut Jean Lamour (UMR CNRS 7198), University of Lorraine, Campus ARTEM, 2 allée André Guinier, 54000 Nancy, France

ABSTRACT

Two alloy compositions, {Co(bal.)-25Cr-0.25C-1Ti} and {Co(bal.)-25Cr- 0.50C-2Ti}, were studied using Thermo-Calc. In parallel the corresponding real alloys were elaborated by foundry and their microstructures, in their as-cast state or after a long stage at 1000 or 1200 °C, were characterized. Thermodynamic calculations and real experiments were globally in good agreement. They both demonstrate that the two alloys are highly refractory, that solidification starts by the crystallization of the alloy matrix in all cases and that all titanium carbides precipitate at the end of solidification and belong to a {matrix + TiC} eutectic compound. The TiC carbides remain stable during long exposure at elevated temperature, for both temperatures for the {0.50C-2Ti}-alloy but only at 1000 °C for the {0.25C-1Ti}-alloy. This observation suggests potential high mechanical properties of the {0.50C-2Ti}-alloy at elevated temperature. Many of the collected experimental data – temperature range of melting or solidification, microstructures stabilized at high temperature (natures, fractions and chemical compositions of the phases) – will be of interest for testing and improving databases.

1. Introduction

Superalloys are refractory metallic alloys used for high temperature applications, such as static or rotating blades in aero-engines and energy-generation turbines [1,2]. Among the most modern ones there are the nickel-based gamma / gamma prime single crystal alloys [3] which are certainly the best ones in term of mechanical [3] and chemical [4,5] resistances at elevated temperatures. However γ/γ' single crystals cannot be easily shaped for obtaining compact pieces. Conventionally cast pieces constituted of equi-axed superalloys remain of great interest. Some attention must be focused on recent formulae of chromium-rich cobalt-based alloys, involving interdendritic script-like shaped TaC [6] or HfC [7]. Such interdendritic carbides which form a eutectic compound with matrix at the end of solidification and which remain stable at elevated temperature, possess additionally a morphology which is recognized as particularly efficient for strengthening alloys at high temperature [8]. This was recently demonstrated by the observation of significant creep resistance at temperatures as high as 1200 °C [9]. Unfortunately such elements (Ta, Hf…) are rather expensive and their high atomic masses tend increasing the density of alloys, which is harmful for transportation applications as well as for industrial pieces in high speed rotation during working.

TiC is also a MC-type carbide. It is formed from an element which is not so refractory as Ta or Hf. Indeed the melting point of Ti is 1725 °C against 2996 °C for Ta or 2205 °C for Hf [10]. TiC is however a very refractory compound, with a melting point of more than 3000 °C [11]. Titanium is an element which is rather cheap and profuse on earth and the MC carbides which can be obtained from Ti is of a rather low density (4.93 g cm^{-3} for TiC against 12.6 and 14.3 for HfC and TaC respectively [11]). The titanium monocarbide is thus potentially very interesting and it is judicious to investigate how it may appear in chromium-rich cobalt-based alloys, where in the microstructure and with which morphology, and how it behaves at high temperature for long-time exposures.

In this work two Co-based compositions involving rather high amounts in titanium and carbon were first studied using thermodynamic calculations to obtain preliminary data about the appearance or not of TiC during solidification and, if TiC can be present, to value the stability of this carbide at high temperature. Thereafter elaborations by casting under inert atmosphere were carried out to obtain the two alloys. Their melting ranges were measured and their microstructures, in their as-cast state or after 46 h isothermally spent at 1000, 1100 and 1200 °C, were characterized. Comparisons will be done between the results of thermodynamic calculations and the real experiments.

---

* Corresponding author.
E-mail address: patrice.berthod@centraliens-lille.org (P. Berthod).

2. Experimental method

2.1. Thermodynamic calculations

Preliminary thermodynamic calculations were carried out using the Thermo-Calc (version N) software [12] working with a database based on the SSOL commercial one [13] especially enriched by Sylvain Michon [14] for the needs of his doctoral research. This database contains the descriptions of the Co-Cr [13], Co-C [13], Cr-C [13], Co-Ti [15], Cr-Ti [16] and Ti-C [17] binary systems as well of the Co-Cr-C [13], Co-Ti-C [18] and Cr-C-Ti [19] ternary systems. Calculations were carried out at successive temperatures between 2000 and 1000 K, interval covering the temperature range of solidification or melting and the solid state temperature range in which diffusion and transformation rates are known to be reasonably possible for usual practical cooling rates. The number of the phases existing at each temperature step, their natures and their mass fractions were noted.

Additional calculations were done at 1000 and 1200 °C for specifying more extensively the metallurgical states of the alloys, for specifying again the natures and mass fractions of the different existing phases, and also their chemical compositions (essentially liquid and matrix). These mass fractions were converted into volume fractions according to Eq. (1) in order to allow thereafter comparisons with the experimental surface fractions measured in the aged samples:

$$f_v[\varphi j] = \left(f_w[\varphi j]/\rho_{\varphi j} \right) \Big/ \sum_i (f_w[\varphi i]/\rho_{\varphi i}) \tag{1}$$

in which $f_v[\varphi j]$, $f_w[\varphi j]$ and $\rho_{\varphi j}$ are respectively the volume fraction, the mass fraction and the density of the phase φ_j. The values taken for the densities were 4.93 g cm^{-3} for the TiC carbides, 6.95 g cm^{-3} for the chromium carbides (Cr_7C_3 and $Cr_{23}C_6$ are almost of the same density), and 8.34, 8.14 and 8.19 g cm^{-3} for the matrixes of the Co-25Cr-0.25C-1Ti and Co-25Cr-0.50C-2Ti alloys respectively. The densities of the alloys were calculated from the mass and dimensions of very regular parallelepipeds accurately cut and measured in the two ingots. The densities of the matrixes were assumed to be very close to the ones of the alloys.

2.2. Synthesis of the alloys

The two alloys were elaborated by high frequency induction foundry (CELES furnace, France) from small parts of pure elements: Co, Cr, Ti, and graphite (Alfa Aesar, all > 99.9 wt% in purity). In each case the parts were placed in a copper crucible internally cooled by room temperature water circulation. A silica tube was placed surrounding the crucible and inside the copper induction coil (also cooled by internal water circulation) to isolate the crucible and the metallic parts from outside. Pumping until reaching about 0.03 millibars was realized three times, each time followed by introduction of pure argon until reaching about 300 millibars. After final pumping, an atmosphere of 300 millibars of argon was present in the fusion chamber. The voltage was increasingly applied until reaching the temperature level which was demonstrated by the preliminary thermodynamic calculations as compulsory for the fusion of the considered alloys as well as for the steady molten state of the obtained liquid alloy. The voltage was maintained at this value (5 kV, frequency: about 110 kHz) during five minutes. The cooling at the end of the isothermal stage cooling was realized, with a rate defined by the rate of power decrease. This procedure led to two ingots of a compact shape, each weighing about 40 g.

2.3. Microstructure characterization of the as-cast state

The ingots were cut using a Delta Buelher saw. A part from each of them was embedded in a cold resin mixture (resin CY230 and hardener HY956 from ESCIL, France). The mounted samples were thereafter ground with SiC papers, for grade varying from 80 to 4000. They were immersed in water and ultrasonically cleaned. Final polishing was realized using a textile disk enriched with 1 μm diamond particles, until obtaining a mirror-like state.

The alloys were observed using Scanning Electron Microscopy (SEM, JEOL JSM-6010A) in Back Scattered Electrons mode (BSE). The general chemical composition of the alloys was verified by Energy Dispersion Spectrometry (EDS) using the EDS device equipping the SEM. Spot EDS measurements were additionally carried out to specify the chemical compositions of the present phases: accurate composition of matrix but only qualitative composition of the different types of particles (too small size to be accurately analyzed). The particles containing especially high contents in carbon and titanium were assumed to be TiC carbides and the ones appearing particularly rich in carbon and chromium were supposed to be chromium carbides (but without further information about their stoichiometry).

2.4. Isothermal exposures of the alloys and metallographic characterization

In both ingots a small parallelepiped was cut in order to carry out differential thermal analysis using a SETARAM TG-DTA apparatus, respecting the following cycle: heating from the ambient temperature up to 1200 °C at + 20 K/min, heating from 1200 °C to 1470 °C at + 5 K/min, cooling down to 1200 °C at −5K/min then at −20K/min. The temperatures of heat absorption start and end and the temperature of heat release start and end were noted on the obtained curves (temperatures at which the heat flow curves took off from the base line - or tangent line - or at which they rejoined again the base line).

2.5. Isothermal exposures of the alloys and metallographic characterization

In each ingot two additional parts were cut for performing the isothermal exposures in high temperature resistance tubular furnace. Their approximate dimensions were 10 mm × 10 mm × 3 mm. After heating at + 20 K/min they were maintained at two high temperatures (1000 and 1200 °C) for 46 h in each case. Post-isothermal cooling was realized at −5 K min^{-1} down to room temperature. Thereafter, these different aged samples were prepared (cutting, embedding, grinding, polishing) and characterized (SEM/BSE observations and photographs, EDS identification of the different types of particles and spot analyses of the chemical composition of the matrix) as previously described for the as-cast alloys. The microstructure characterization was completed by the measurements of the surface fractions of the phases using the image analysis tool of the Photoshop CS software (Adobe).

2.6. Hardness measurements

The as-cast alloys as well as the aged ones were all subjected to Vickers indentation under a load of 10 kg, in order to correlate with the observed carbides surface fractions and to qualitatively anticipate about their possible mechanical potential at high temperature. The used apparatus was a Testwell Wolpert macro-indentor.

3. Results and discussion

3.1. Thermodynamic calculations

The first results of thermodynamic calculations are presented in Fig. 1 and in Fig. 2. Fig. 1 allows knowing qualitatively the solidification and solid state transformations of the Co-25Cr-0.25C-1Ti alloy during cooling from the liquid state and until reaching 1000 K. In the case of Fig. 2 the same transformations, but concerning the Co-25Cr-0.50C-2Ti alloy, can be qualitatively anticipated. Obviously the two alloys would begin their solidification by the crystallization of the FCC matrix. This first stage of crystallization is expected to be a little longer for the first alloy than for the second one since the temperature range is
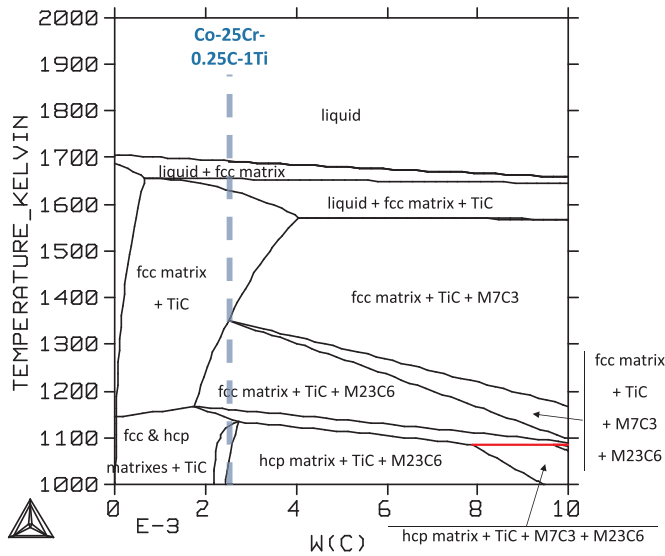
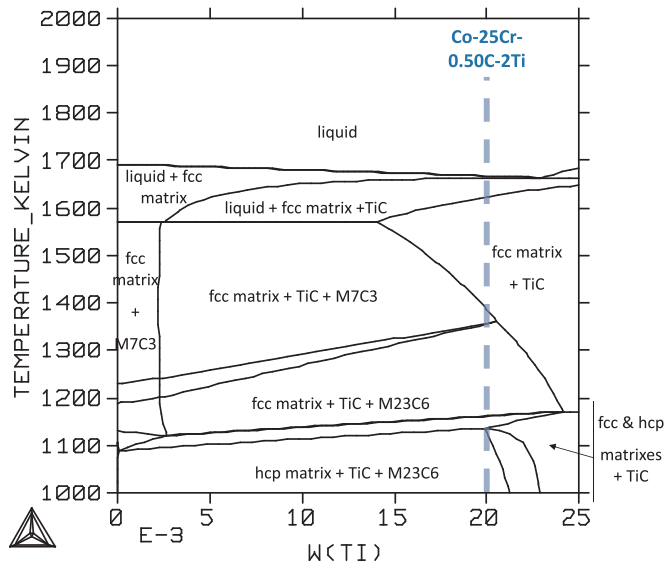**Fig. 1.** The {25 wt%Cr-1 wt%Ti}-section computed with Thermo-Calc with position of the low carbides alloy.

Fig. 2. The {25 wt%Cr-0.50 wt%C}-section computed with Thermo-Calc with position of the high carbides alloy.

Fig. 3. The solidification of the Co-25Cr-0.25C-1Ti alloy computed with Thermo-Calc.

Fig. 4. The solidification of the Co-25Cr-0.50C-2Ti alloy computed with Thermo-Calc.

broader in the first case than in the second one. Qualitatively one can think to a more developed pre-eutectic dendrite network for the {0.25C-1Ti}-alloy than for the {0.50C-2Ti}-alloy. Inversely the later alloy will probably contain a more extended interdendritic domain composed of the {matrix + TiC} eutectic than the former one. Indeed, the eutectic precipitation of matrix and TiC carbides which will effectively take over from the pre-eutectic crystallization of matrix, will take place during a cooling over a much wider temperature range (more than 200 K against only several tens K for the {0.25C-1Ti}-alloy). After total solidification the metallurgical state can be double-phased (matrix + TiC) for these two alloys with equal atomic contents between carbon and titanium. During the subsequent solid state cooling of the Co-25Cr-0.25C-1Ti alloy, $M_{23}C_6$ carbides would start precipitating after several hundreds of Kelvin under the end of solidification. Its next solid state transformation should be the allotropic change of the austenitic FCC matrix into a hexagonal compact HCP one. This is globally the same scenario for the Co-25Cr-0.50C-2Ti.

The theoretic solidifications and the solid state transformations at temperatures still high are represented more quantitatively for the two
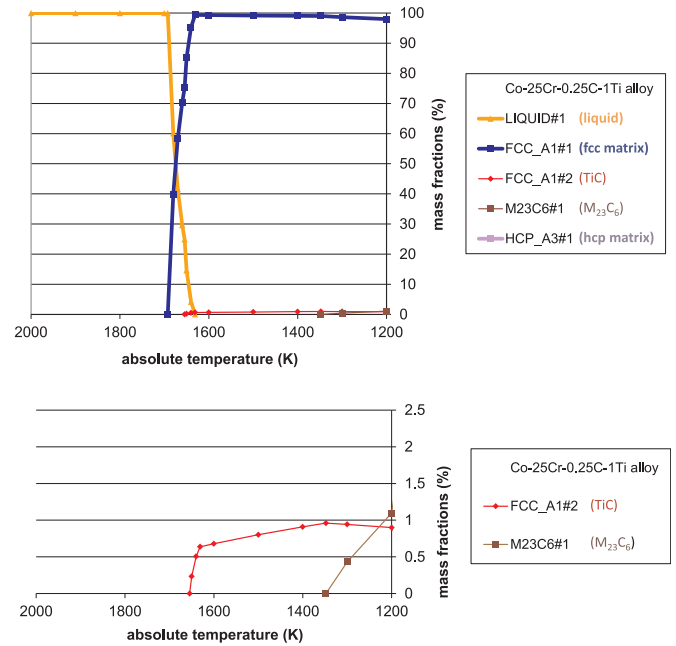
alloys in Fig. 3 (Co-25Cr-0.25C-1Ti) and Fig. 4 (Co-25Cr-0.50C-2Ti). In each case the top graph concerns all phases while the bottom graph, enlarged version of the previous one, only concerns carbides. One logically finds confirmation that the first carbide to appear is the titanium one (TiC, FCC_A1#2), while chromium carbides may precipitate in solid state more 200 K lower than the appearance of the titanium carbides. TiC carbides initially precipitate during the eutectic part of solidification until reaching a little more than 0.5 mass.% for the {0.25C-1Ti}-alloy and almost 2 mass.% for the {0.50C-2Ti}-alloy. In both cases titanium carbides stay alone before the solid state precipitation of the chromium carbides, directly $Cr_{23}C_6$ for the first alloy and seemingly with a short transition of Cr_7C_3 before $Cr_{23}C_6$ for the second one. The
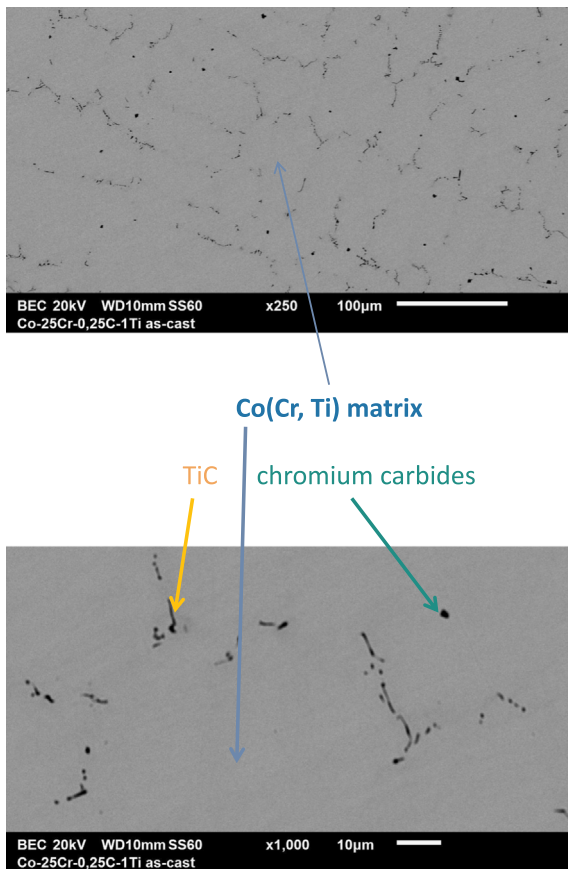
Fig. 5. The as-cast microstructure of the Co-25Cr-0.25C-1Ti alloy (top: general view, bottom: detailed view).

Fig. 6. The as-cast microstructure of the Co-25Cr-0.50C-2Ti alloy (top: general view, bottom: detailed view).

predicted mass fractions in chromium carbides are lower than the TiC ones but of the same order of magnitude.

3.2. As-cast microstructures of the obtained alloys

After elaboration of the alloys by high frequency induction melting and metallographic preparation of parts cut in the obtained ingots, microstructure examination in electron microscopy was carried out to have a look to the as-cast microstructures. Two micrographs, presented in Fig. 5, illustrate the microstructure of the as-cast {0.25C-1Ti}-alloy, with two magnifications. This alloy is obviously composed of a dendritic matrix (solid solution of Co containing Cr and a part of Ti and of C) and of interdendritic dark particles. These ones are rich in titanium and in carbon. The same type of microstructure is presented by the {0.50C-2Ti}-alloy (Fig. 6), with more interdendritic particles. In this second alloy these particles are either rich in Ti and C, or in chromium and C. Because of the too low surface fraction of these precipitates and of their too low size, even in the second alloy, neither X-ray diffraction nor spot chemical analysis by energy dispersion spectrometry and by wavelength dispersion spectrometry allowed to accurately specify the nature of these particles. They were only identified as being rich in Ti and C for some of them and in Cr and C for the other ones.

3.3. Melting temperature range of the obtained alloys

In parallel with the preparation of the metallographic samples small parallelepipeds were cut in the ingots to perform differential thermal analysis. The obtained DTA curves are displayed in Figs. 7 and 8, for respectively the {0.25C-1Ti}-alloy and the {0.50C-2Ti}-alloy. The first alloy starts melting at about 1370 °C and finishes melting above 1460 °C. It starts solidifying at about 1400 °C, obviously after an
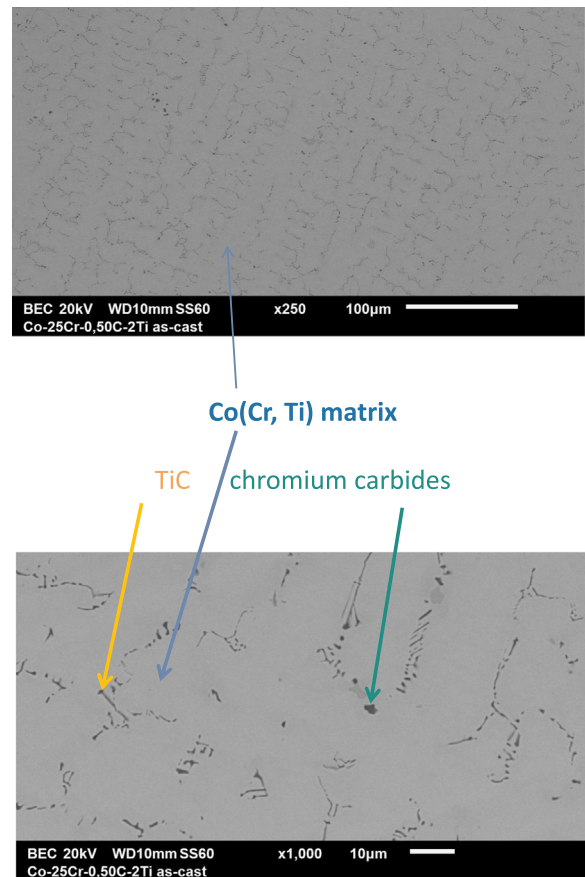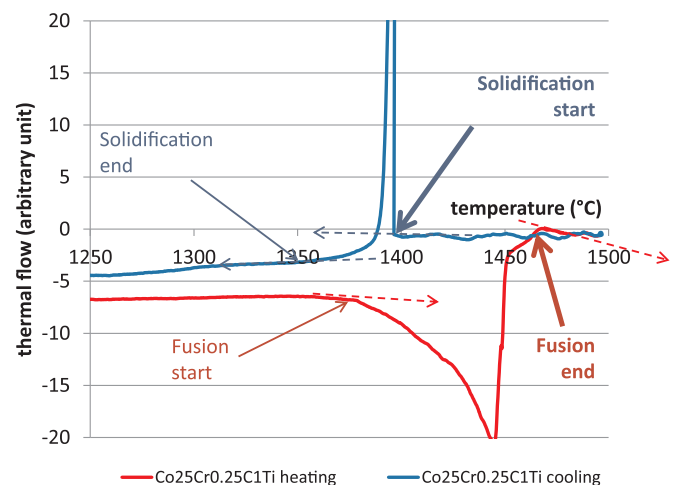

Fig. 7. The DTA curve obtained for the Co-25Cr-0.25C-1Ti alloy.

important undercooling as suggested by the sudden crystallization releasing a great quantity of heat over a small temperature range. It finishes its solidification near 1350 °C. The melting of the second alloy starts at a temperature lower than for the first one, at about 1270 °C, and finishes at about 1450 °C. An undercooling is also observed prior to the start of its solidification, revealed by a jump in released heat at about 1420 °C. The end of solidification happens just below 1300 °C.

The exact values of melting and solidification starts and ends determined by DTA for the {0.25C-1Ti}-alloy are given in Table 1, with the corresponding values of solidus and liquidus temperatures issued from thermodynamic calculations. One can note that the calculated
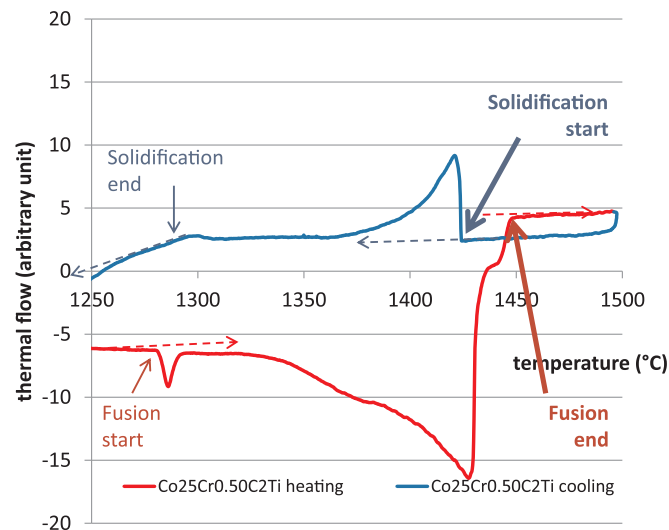
Fig. 8. The DTA curve obtained for the Co-25Cr-0.50C-2Ti alloy.

Table 1
Comparison of the calculated liquidus and solidus temperatures and the measured ones for the Co-25-0.25C-1Ti alloy.

Thermo-Calc	Differential thermal analysis	Consistent?
Liquidus temperature (°C)	Fusion end's temperature (°C)	Yes / No
	Average value (°C)	
	Solidification start's temperature (°C)	
1419	1464	**YES**
	1432	
	1399	
Solidus temperature (°C)	Fusion start's temperature (°C)	Yes / No
	Average value (°C)	
	Solidification end's temperature (°C)	
1358	1375	**YES**
	1365	
	1354	

solidus and liquidus are in good agreement with the one deduced from the DTA results.

In contrast, the calculated and experimental results are not consistent for the {0.50C-2Ti}-alloy (Table 2). The calculated solidus temperature is much higher than the melting start's and solidification end's ones, as well as the average of the two. The calculated liquidus temperature is significantly lower than the melting end's temperature, the solidification start's one and the average value.

Table 2
Comparison of the calculated liquidus and solidus temperatures and the measured ones for the Co-25-0.50C-2Ti alloy.

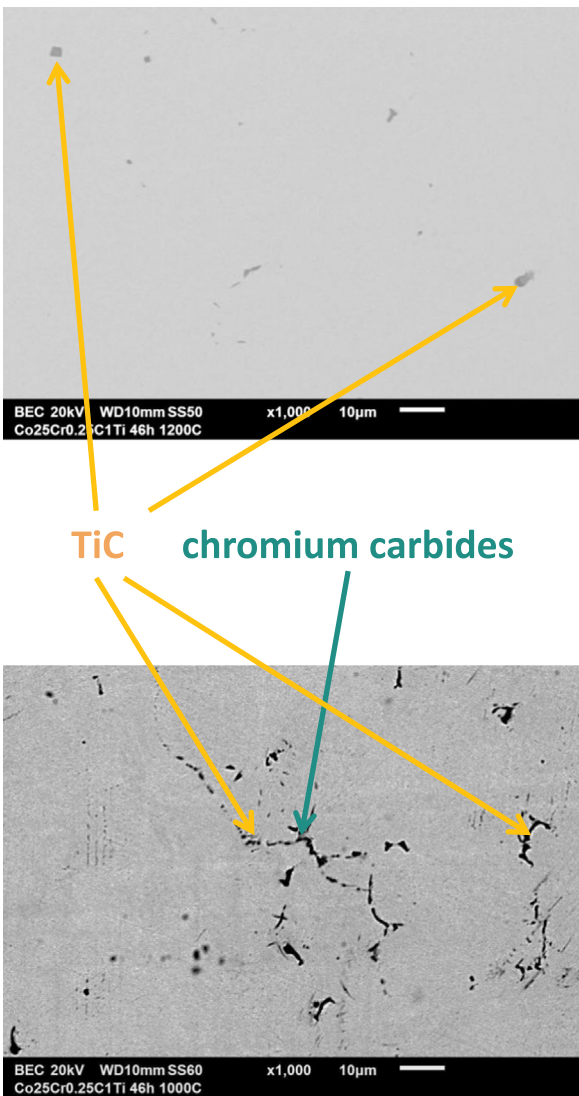| Thermo-Calc	Differential thermal analysis	Consistent?
Liquidus temperature (°C)	Fusion end's temperature (°C)	Yes / No
	Average value (°C)	
	Solidification start's temperature (°C)	
1394	1447	**NO**
	1438	
	1428	
Solidus temperature (°C)	Fusion start's temperature (°C)	Yes / No
	Average value (°C)	
	Solidification end's temperature (°C)	
1351	1278	**NO**
	1284	
	1290	

Fig. 9. The microstructures of the Co-25Cr-0.25C-1Ti alloy aged at 1200 °C (top) and 1000 °C (bottom).

3.4. Aged microstructures

The microstructure behaviors of the two alloys when isothermally exposed at high temperature were studied at 1000 and 1200 °C during 46 h. The highest temperature was considered as possible according to the DTA measurements which previously demonstrated that none of the two alloys risks melting. The aged microstructures were analyzed following the same protocol of preparation and characterization as the as-cast samples. By looking to the micrographs presented in Fig. 9 it appears that, during the stay at 1200 °C, the {0.25C-1Ti}-alloy has become almost single-phased. Indeed it has lost almost all its initial carbides, obviously dissociated and their constitutive elements dissolved in the solid solution. One can see here and there some rare TiC carbides as isolated blocky particles. After 46 h spent at 1000 °C, the carbides are still here but they obviously coalesced. One can distinguish black/dark gray TiC carbides and pale gray chromium carbides, for the chosen contrast and brightness settings. During the same tests the {0.50C-2Ti}-alloy behaved differently (Fig. 10). For both temperatures the surface fraction of carbides was not so lowered. The TiC carbides were a little fragmented and coalesced after exposure at 1200 °C while chromium carbides are difficult to see or do not exist anymore. Both carbides are still present after exposure at 1000 °C. The dark TiC carbides obviously staid script-like shaped. The chromium carbides are dispersed as rare
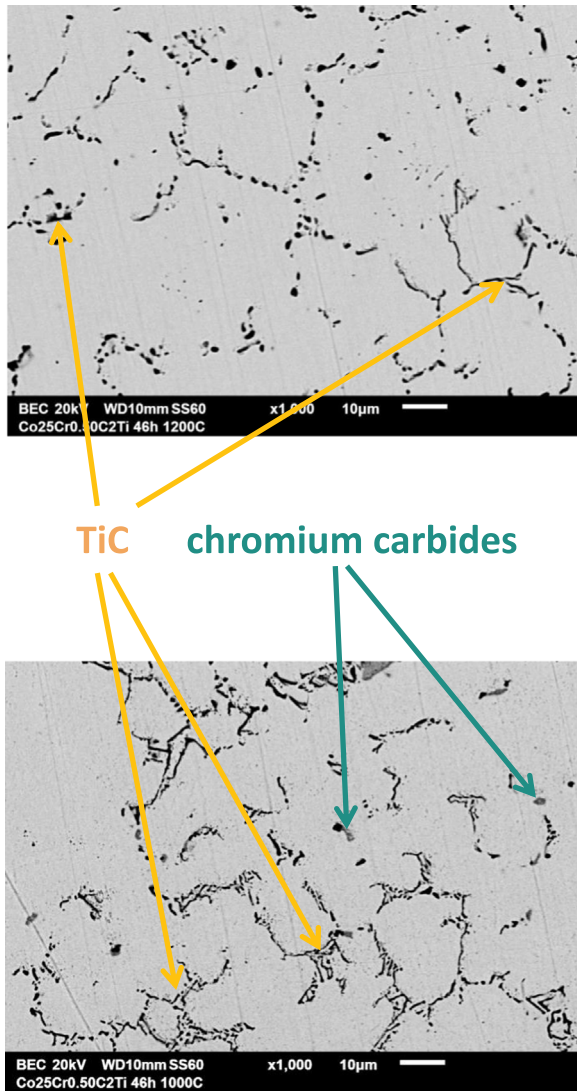
Fig. 10. The microstructures of the Co-25Cr-0.50C-2Ti alloy aged at 1200 °C (top) and 1000 °C (bottom).

blocky pale particles.

3.5. Metallurgical state comparison between calculations and experiments

The theoretic results issued from thermodynamic calculations and the ones issued from metallographic characterization may be compared in the fields of carbides natures, carbides fractions and matrixes

chemical compositions. This was done for the {0.25C-1Ti}-alloy in Table 3 and for the {0.50C-2Ti}-alloy in Table 4.

Concerning the first alloy rather good agreement is found concerning the chemical composition of the matrix. The calculated and measured chromium contents are very close to one another. In contrast, the titanium content measured by EDS seems being a little higher in the aged alloys than the predicted values. This suggests that a lower fraction of TiC carbides remain stable in the microstructure by comparison with predictions. This is exactly the case: the TiC are effectively less present in the aged samples than anticipated by calculations. This is particularly true for 1200 °C, temperature at which TiC were expected to be still present with rather high fraction (1.4 vol%), just a little less than for 1000 °C: only less than 0.3 vol% of TiC staid in the 1200 °C-aged {0.25C-1Ti}-alloy. Concerning the chromium carbides, excellent agreement appears between calculations and experiment for 1200 °C: they are totally absent according to calculations and to metallography. Differences appear for 1000 °C but the fractions in chromium carbides are close to 0 in both cases.

The same good correspondence of the chromium content in matrix and the same type of difference in titanium content as for the first alloy is found again concerning the chemical composition of the matrix of the second alloy after aging at 1200 and 1000 °C: the Cr contents are almost equal and the Ti content tends to be higher in the real alloy than the calculated values. Curiously, the volume fractions of the TiC carbides are higher in the aged real alloy than the calculated values. The same hierarchy is found for the chromium carbides at 1000 °C: their surface fraction in the microstructure is higher than their calculated volume fraction. For 1200 °C, calculations and metallography led to the same results: total absence of chromium carbides.

3.6. Hardness

The average and standard deviation values of the five indentation results obtained for each {alloy, state} couple are given in Table 5. The aging at 1000 °C transformed the {0.25C-1Ti}-alloy in a harder material, seemingly thanks to the previously observed coalescence of the carbides occurred during the aging. Inversely, the hardness falls under the as-cast alloy value after aging at 1200 °C, consecutively to the disappearance of all carbides. For all states the {0.50C-2Ti}-alloy is harder than the first one. The equivalent hardness for the as-cast state and for the 1000 °C-aged state can be easily related to the unmodified carbide network. The softening observed after 46 h at 1200 °C can be also easily explained by the decrease in carbide fraction and by the fragmentation of the TiC carbides. The hardness of the 1200 °C-aged {0.50C-2Ti}-alloy nevertheless remains higher than the one of the as-cast {0.25C-1Ti}-alloy.

4. Discussion

Titanium, as many other MC-former elements, is stronger in this role

Table 3
Comparison of the metallurgical states at 1200 and 1000 °C of the Co-25Cr-0.25C-1Ti alloy as calculated by Thermo-Calc (Th.-Calc) and as really obtained (Exp.).

Temperature	FCC Co-based matrix		TiC carbide		$M_{23}C_6$ carbide	
Source:	Th.-Calc	Exp.	Th.-Calc	Exp.	Th.-Calc	Exp.
1473.15 K (1200 °C)	Chem. compo: 74.365 Co 25.192 Cr 0.345 Ti 0.098C	wt% in Cr and Ti: Bal. 25.4 ± 0.5 0.6 ± 0.1 Not meas.	0.832 mass.% i.e. 1.400 vol%	average ± std dev (surf.%) 0.26 ± 0.07	/	/
1273.15 K (1000 °C)	Chem. compo: 74.801 Co 24.896 Cr 0.260 Ti 0.043C	wt% in Cr and Ti: Bal. 24.7 ± 0.3 0.4 ± 0.2 Not meas.	0.933 mass.% i.e. 1.566 vol%	average ± std dev (surf.%) 1.37 ± 0.17	0.637 mass.% i.e. 0.758 vol%	average ± std dev (surf.%) 0.17 ± 0.30

Table 4

Comparison of the metallurgical states at 1200 and 1000 °C of the Co-25Cr-0.50C-2Ti alloy as calculated by Thermo-Calc (Th.-Calc) and as really obtained (Exp.).

Temperature	FCC Co-based matrix		TiC carbide		[a]M₇C₃ or [b]M₂₃C₆ carb.	
Source:	Th.-Calc	Exp.	Th.-Calc	Exp.	Th.-Calc	Exp.
1473.15 K (1200 °C)	Chem. compo: 74.081 Co 25.497 Cr 0.314 Ti 0.108C	wt% in Cr and Ti: Bal. 25.7 ± 0.2 0.5 ± 0.1 Not meas.	2.145 mass.% i.e. 3.512 vol%	average ± std dev (surf.%) 6.11 ± 0.28	/	/
1273.15 K (1000 °C)	Chem. compo: 74.679 Co 25.017 Cr 0.261 Ti 0.043C	wt% in Cr and Ti: Bal. 25.0 ± 0.3 0.8 ± 0.3 Not meas.	2.189 mass.% i.e. 3.577 vol%	average ± std dev (surf.%) 4.55 ± 1.05	[b]0.983 mass.% i.e. 1.139 vol%	average ± std dev (surf.%) 1.99 ± 1.82

Table 5

Room temperature hardness of the two alloys in their three states (as-cast or aged at one of the two temperatures).

Vickers 10 kg (10 indentations)	Co-25Cr-0.25C-1Ti	Co-25Cr-0.50C-2Ti
After 46 h at 1200 °C	263 ± 12	317 ± 5
After 46 h at 1000 °C	331 ± 12	362 ± 13
As-cast	306 ± 21	364 ± 12

than chromium, according to the carbides' Ellingham diagram [20–22]. This was thus not a surprise to note that TiC formed at the expense of chromium carbides in the alloys considered in this work, observations here predicted in a first time with thermodynamic calculations and directly done on really elaborated alloys in a second time.

However, this was not self-evident as earlier seen in the case of tantalum carbides in nickel-based alloys. Indeed, TaC carbides were effectively present at the expense of chromium carbides in cobalt-chromium alloys [6] while they were replaced by chromium carbides in nickel-chromium alloys [23]. A problem of lack of thermodynamic stability of TiC in presence of chromium was encountered in nickel-based alloys, for example in [24]. It was thus not sure that TiC is able to compete with chromium carbides in the present alloy, even if a cobalt-base previously favored another MC carbide (TaC, [6]) at the detriment of chromium carbides in contrast with what occurred in nickel-based alloys [20].

The preliminary calculations performed here suggested the successful formation of TiC carbides during solidification and their high stability at elevated temperature. During cooling from the liquid state they are the second solid phase to crystallize (after the matrix), and the single carbide phase to appear during solidification. Chromium carbides are expected to appear in a second time, at lower temperatures, by solid state precipitation. This theoretic succession of phase transformations during cooling is common to the two alloys. The main difference concerns the quantities of carbides which are not the same (logically higher for the second alloy than for the first one, regarding their respective contents in C). These previsions are globally confirmed by the as-cast microstructures: dendritic matrix (thus necessarily the first phase to crystallize) and eutectic shape of the TiC carbides (script-like mixed with matrix). The chromium carbides look like solid state precipitates. After isothermal exposure at high temperature long enough to expect the reaching of the thermodynamic equilibria, it appeared that the TiC carbides became and remained the single carbide present at 1200 °C and the two carbides still existed after exposure at 1000 °C. Calculations and experiment results thus appeared as qualitatively consistent. Image analysis allowed to possibly give quantitative confirmation of this good agreement. This was not really the case since the volume fractions of the two types of carbides issued from the mass fractions issued from thermodynamic calculations and the ones deduced from the surface fractions measured by Adobe Photoshop corresponded to one another more or less imperfectly. The fineness of the script-like eutectic TiC and the small size of the chromium carbides, as well as the proximity of the tint of the later ones with the matrix, may be responsible of this mismatch. It is true that, in spite of the care with which the threshold was rated, the surface fractions of carbides were measured without a high accuracy. Some of the standard deviation values witness of these difficulties. Another significant lack of consistency between calculations and experimental measurements was found concerning some of the DTA results. This was the case of the {0.50C-2Ti}-alloy for which the melting or solidification range was more extended that the difference of the calculated solidus and liquidus temperatures. This suggests that the database merits to be improved for the C-richest Ti-richest part of the diagram at high temperature. For instance, the description of the Co-Cr-Ti ternary system, which is currently lacking in our database, may be incorporated rather shortly since first results concerning this system start to be available, as the ones obtained by P. Zhou et al. rather recently published [25]. Anyway one must consider that, in its present state, this database is globally performing enough to give very useful indication on the microstructure of Ti-containing Cr-rich cobalt-based alloys containing carbon for forming carbides.

5. Conclusions

Cobalt-based alloys elaborated by classical foundry keep significant interest for many applications at high temperature and, besides solid solution strengthening, the necessity to strengthen grain boundaries and to consolidate the inter-dendrites cohesion leads to favor the long term presence of particles such as script-like shaped eutectic carbides. TiC carbides, which correspond to these requirements, may be more interesting than other MC carbides thanks to their lower density and for the availability of titanium much more extended than the one of other MC-former elements. Although obtaining successfully stable TiC carbides was previously showed as not possible in nickel-chromium alloys, both by thermodynamic calculations and real experiments, the same types of investigations undertaken in the present study both just demonstrate that this is totally different in cobalt-chromium alloys. With the two alloys of this type considered in the present work, preliminary calculations, carried out using a home-made database, suggested in a first time that obtaining eutectic TiC carbides is possible. In a second time, the elaboration of real alloys led to as-cast microstructures with predominant TiC carbides. Furthermore these ones did not accidentally precipitated during the rather fast solidification (and thus in non-equilibrium conditions) since they remained stable at high temperature as showed by isothermal aging applied on rather long time. This is true that this is essentially the alloy with 050 wt%C and 2 wt%Ti which staid really stable in these conditions. The rather high room temperature hardness of this alloy in its as-cast state as well as after several days spent at high temperatures suggests interesting mechanical properties at elevated temperatures. Unfortunately, with its current chemical composition this alloy obviously starts melting at a temperature a little

too low to expect high creep resistance at elevated temperature. This is probably due to the presence of some rare chromium carbides that the respect of the atomic equality of titanium and carbon did not succeed to totally avoid the formation of these carbides responsible of low melting point of the grain boundaries. However, by considering the isopleth sections presented in the first figures of this manuscript, it seems possible to suppress the chromium carbides for example by increasing the Ti content up to 2.4 wt% for the same C content (0.50 wt%).

However one must be careful with such deductions made from the current database since, even if good predictions were made by using it for the thermodynamic calculations, this one may lead to slight discrepancies, as the ones observed in the present study, notably in the case of this {0.50C-2Ti}-alloy. It is preferable to improve the accuracy of this database prior using it for designing new TiC-containing cobalt-chromium alloys, notably by using the presented metallographic data obtained in this work. These ones are also available to test other databases and to serve as references for improving them for better predictions if necessary.

Appendix A. Supporting information

Supplementary data associated with this article can be found in the online version at doi:10.1016/j.calphad.2019.02.009.

References

[1] C.T. Sims, W.C. Hagel, The Superalloys, John Wiley & Sons, New York, 1972.
[2] E.F. Bradley, Superalloys: A Technical Guide, ASM International, Metals Park, 1988.
[3] M.J. Donachie, S.J. Donachie, Superalloys: A Technical Guide, 2nd ed., ASM International, Materials Park, 2002.
[4] P. Kofstad, High Temperature Corrosion, Elsevier applied science, London, 1988.
[5] D.J. Young, High Temperature Oxidation and Corrosion, Elsevier Corrosion Series, Amsterdam, 2008.
[6] P. Berthod, S. Michon, L. Aranda, S. Mathieu, J.C. Gachon, Calphad 27 (2003) 353–359.
[7] P. Berthod, E. Conrath, Mater. Chem. Phys. 143 (2014) 1139–1148.
[8] P. Berthod, J. Alloy. Compd. 481 (2009) 746–754.
[9] P. Berthod, E. Conrath, J. Mater. Sci. Technol. Res. 1 (2014) 7–14.
[10] P.T.B. Shaffer, High-Temperature Materials – N°1 Materials Index, Plenum Press, New York, 1964.
[11] G.V. Samsonov, High-Temperature Materials – N°2 Properties Index, Plenum Press, New York, 1964.
[12] Thermo-Calc version N: "Foundation for Computational Thermodynamics" Stockholm, Sweden, Copyright (1993, 2000). ⟨www.thermocalc.com⟩.
[13] SSOL database, SGTE Solutions Database, Scientific Group Thermodata Europe, Bo Sundman, Stockholm, Sweden
[14] S. Michon, Metallurgical and Mechanical Optimization of Cobalt-based Superalloys for Glass-forming at 1200 °C (Ph.D. thesis), University Henri Poincaré Nancy 1, Vandoeuvre-lès-Nancy, 2004.
[15] G. Cacciamani, R. Ferro, I. Ansara, N. Dupin, Intermetallics 8 (2000) 213–222.
[16] W. Zhuang, J. Shen, Y. Liu, L. Ling, S. Shang, Y. Du, J.C. Schuster, Z. Metallkd. 91 (2000) 121–127.
[17] S. Jonsson, Z. Metallkd. 87 (1996) 703–712.
[18] L. Dumitrescu, M. Ekroth, B. Jansson, Metall. Mater. Trans. 32A (2001) 2167–2174.
[19] J. Schuster, Y. Du, Calphad 23 (1999) 393–408.
[20] S.R. Shatynski, Oxid. Met. 13 (2) (1979) 105–118.
[21] P. Berthod, Adv. Mater. Sci. Eng. (2017), https://doi.org/10.1155/2017/4145369 (Article ID 4145369, 9 pages).
[22] P. Berthod, Riv. Ital. della Saldatura 4 (2017) 477–490.
[23] P. Berthod, L. Aranda, C. Vébert, S. Michon, Calphad 28 (2004) 159–166.
[24] P. Berthod, E. Kretz, F. Allègre, Calphad 56 (2017) 41–48.
[25] P. Zhou, Y. Peng, B. Hu, S. Liu, Y. Du, S. Wang, G. Wen, W. Xie, Calphad 41 (2013) 42–49.